Engineering Conferences International
ECI Digital Archives

5th International Conference on Porous Media and Their Applications in Science, Engineering and Industry

Refereed Proceedings

Summer 6-26-2014

Turbulence in porous media: Some fundamental questions addressed by DNS solutions

Marc Florian Uth
Hamburg University of Technology

Y. JIn
Hamburg University of Technology

A. V. Kuznetsov
North Carolina State University at Raleigh

H. Herwig
Hamburg University of Technology

Proceedings of the 5th International Conference on Porous Media and its Applications in Science and Engineering
ICPM5
June 22-27, 2014, Kona, Hawaii

TURBULENCE IN POROUS MEDIA: SOME FUNDAMENTAL QUESTIONS ADDRESSED BY DNS SOLUTIONS

M.F. Uth[(a)], Y. Jin[(a)], A.V. Kuznetsov[(b)] and H. Herwig[(a)]
[(a)] *Institute of Thermo-Fluid Dynamics, Hamburg University of Technology, Hamburg ,D-21073, Germany*
[(b)] *Dept. of Mechanical and Aerospace Engineering, North Carolina State University, Raleigh, NC 27695-7910, USA*

ABSTRACT
In a generic porous matrix built by a large number of rectangular bars the flow is determined numerically by a DNS approach. Turbulent flow is thus simulated avoiding modelling in order to decide whether turbulent structures with scales much larger than the pore scale exist. So far only under-resolved DNS solutions are determined from which, however, definite conclusions with respect to the maximum turbulent length scale can be drawn.

INTRODUCTION
A flow in porous media is characterized by length scales of different magnitude. Assuming continuous fluid flow, i.e. no influence of the molecular nature of the fluid, the smallest relevant geometrical scale is the pore scale which typically can be an average hydraulic diameter of the pores. Next in the hierarchy of scales comes the size of a representative elementary volume (REV) in cases where pores are of very different individual size. For a homogeneous matrix with a regular pore structure of unique size in the Darcy flow regime this REV is of the order of the pore size itself.
These considerations are important when it comes to the question of turbulent flow in porous media. For high enough pore scale Reynolds numbers there definitely will be a turbulent flow within the pores (since they basically are microchannels) after flow transition when the Reynolds number exceeds the critical Reynolds number of the micro-channel. This is the same situation as for microscopic flows through conduits (again assuming that there are no molecular effects, like slip velocity), see [1] and [2] for further details.
There is, however, a controversy whether macroscopic turbulence with eddy sizes beyond the pore scale exists. From an extensive literature review two widely contradicting points of view can be found. They basically disagree with respect to the question whether or not the solid material of the porous matrix inhibits the formation of macroscopic eddies.
The first view was originally expressed in Nield (1991) [3], p. 271, and then further developed in Nield (2001) [4]. According to this view, true macroscopic turbulence, at least in a dense porous medium, is impossible because of the limitation on the size of turbulent eddies imposed by the pore scale. Thus any turbulence in porous media is restricted to turbulence within the pores.
The second class of models deals primarily with macroscopic turbulence in porous media. Representative models are those developed by Lee and Howell (1987) [5], Prescott and Incropera (1995) [6], and Antohe and Lage (1997) [7].
This crucial question about turbulence in porous media cannot be addressed by RANS (Reynolds averaged equations) and not even by LES (large eddy simulation) since then always turbulence modelling is involved which itself can be questioned. The only way to answer this question without ambiguity is to refer to the experiment or to DNS solutions (DNS: direct numerical simulation of the turbulent flow accounting for all scales up to the Kolmogorov scale). Since measurements within the porous matrix are more than challenging, DNS solutions appear to be the best alternative.
Therefore we performed DNS investigations of the flow through a generic porous matrix described and discussed in the next section.

NOMENCLATURE

d	=	Obstacle size
f	=	Particle distribution function
g_i	=	Prescribed pressure gradient
p	=	Pressure
R_{ij}	=	Two point correlation
$\tilde{R}_{ij}$	=	Pseudo two point correlation
$\hat{R}_{ij}$	=	Turbulent two point correlation
Re	=	Reynolds number
s	=	Pore size
u_i	=	Velocity component
$\vec{x}$	=	Position vector

Greek Symbols

$\bar{\xi}$	=	Particle velocity vector
η	=	Kolmogorov scale
ν	=	Kinematic viscosity

Subscripts

m	=	Mean
c	=	critical

1 The porous matrix

1.1 The representative elementary volume for turbulent flow

The concept of a representative elementary volume (REV) basically means to determine the smallest sub-volume of a porous matrix that shows the same behavior with respect to the flow through it as can be observed in the whole matrix. In the introduction it was argued already that the REV of a regular matrix is of the order of the pore size when the flow is a Darcian flow (low Reynolds number, locally creeping flow) and the matrix is geometrically regular on the pore size. We call this REV-D and in addition introduce a representative elementary volume REV-T. This volume is one in a turbulent flow and will be larger than the REV-D when macroscopic turbulent eddies exist with sizes much larger than the pore size.
The Crucial questions (so far for a regular porous matrix) are:

- Which is the REV-T scale?
- Is the REV-T much larger than the REV-D, i.e. are there macroscopic turbulent eddies in porous media?

1.2 The generic porous matrix for a DNS analysis

With the discussion about turbulence in porous media in mind we designed a generic porous matrix according to the three following assumptions:

(1) The matrix may have a regular structure since the crucial effects on turbulence will not be a consequence of the irregularity of the matrix.

(2) The matrix may be geometrically two dimensional since turbulence which itself is three-dimensional will be affected by the presence of a matrix itself, irrespective of its 2- or 3-dimensional nature.

(3) The porosity in our model is relatively high since smaller porosity will result in stronger suppression of any macroscopic turbulence.

Fig. 1 shows our generic porous matrix (GPM) built by a large number of bars arranged as periodic arrays forming a porous medium. Within this regular geometrical structure a representative volume REV-D is of size 2s while the size of REV-T is yet unknown. A strategy to find the REV-T can be to start with a large number of elementary bars (size: d), calculate the turbulent flow in that domain and then reduce the number of bars systematically. As long as the results in the reduced domain are those of the larger ones a further reduction is appropriate.

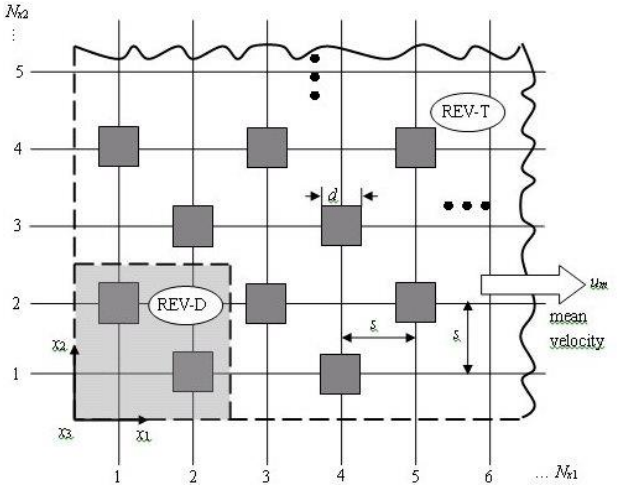

Figure 1: Generic porous matrix (GPM) with the representative elementary volume REV-D and REV-T.

2 DNS calculations in a porous medium

2.1 Preliminary remark

The only way to completely avoid turbulence modelling in CFD solutions (CFD: computational fluid dynamics) is to directly simulate the fluid flow, accounting for all relevant length and time scales. This approach is known as DNS, see [8] for a general introduction. Due to its enormous demand of computational resources (cpu time and storage capacity) only certain benchmark cases, like [9-11], or special fundamental problems like [12~14] can be handled by this method.

2.2 DNS methods

We use two very different numerical methods in order to compare the results as part of a verification procedure and also since they complement each other in certain aspects. They are

- a finite volume method (FVM) to directly solve the Navier-Stokes equations
- a Lattice-Boltzmann method (LBM) to determine the particle distribution which indirectly corresponds to solving the Navier-Stokes equations.

Both methods have been tested against each other in [14] for the problem of a turbulent flow along a rough wall. In [14] wall roughness was composed of two-dimensional bars on an otherwise smooth wall ending up in a geometrical situation which in one dimension is very similar to the porous medium design shown in Fig. 1.

2.2.1 The finite volume method (FVM)

The basic equations to be solved for the incompressible flow of a Newtonian fluid with a finite volume method are the Navier-Stokes equations. In Cartesian coordinates, nondimensionalized with d and u_m and using the Einstein summation convention, they read [15]

$$\frac{\partial u_i}{\partial x_i} = 0 \tag{1}$$

$$\frac{\partial u_i}{\partial t} + \frac{\partial \left(u_i u_j\right)}{\partial x_j} = -\frac{\partial p}{\partial x_i} + \frac{1}{\mathrm{Re}} \frac{\partial^2 u_i}{\partial x_j^2} + g_i \tag{2}$$

Here the Reynolds number is

$$\mathrm{Re} = \frac{u_m d}{\nu} \tag{3}$$

with u_m and d according to Fig. 1 and ν as kinematic viscosity of the fluid.

When (1) – (3) are solved, the solution domain has to be the REV-T, see Fig. 1, extending in the third direction by a length L_3, see the discussion of that in section 3.3. Boundary conditions are periodic in all three directions since the REV-T is an arbitrary cutout with respect to the whole porous matrix. Periodic boundary conditions here mean that all flow quantities (except the pressure in flow direction) are equal on opposing surfaces of the REV-T.

In Eq. (2), g_i is the prescribed pressure gradient by which a particular flow rate is ensured. The solution of Eqs. (1) ~ (3) is advanced in time with the second order implicit backward Euler method. To compute the derivatives of the velocity, the variables at the interfaces of the grid cells are obtained with linear interpolation. With the solutions at the interfaces, a second order central difference scheme is gained for spatial discretization. The pressure at the new time level is determined by the Poisson equation. The velocity is corrected by the Pressure-Implicit with Splitting of Operators (PISO) pressure-velocity coupling scheme.

2.2.2 The Lattice-Boltzmann method (LBM)

This method statistically models the propagation and interaction of particles and thus simulates the flow. For small Mach numbers, the macroscopic velocities which then emerge are solutions of the Navier-Stokes equations.

The basic equation for the LBM is a discretized version of the Boltzmann-Equation for the particle distribution function $f\left(\vec{\xi}, \vec{x}, t\right)$, which reads, see [16]

$$\vec{\xi} \frac{\partial f}{\partial \vec{x}} + \frac{\partial f}{\partial t} = \Theta \tag{4}$$

Here $f\left(\vec{\xi}, \vec{x}, t\right)$ determines the probability to find a particle with velocity $\vec{\xi}$ at a position $\vec{x}$ at a time t. This function f can be modified either by the motion of particles or by their collision which is determined by the collision operator Θ in Eq. (4).

The Lattice-Boltzmann equation as a discretized form of the Boltzmann equation emerges after a discretization of velocity, space and time. For an isotropic behavior of the fluid the space can best be discretized by a uniform Cartesian grid. Then the discretizations of velocity and time have to be such that a particle travels exactly from one grid point to the next neighbor within one time step. Different macroscopic velocities now correspond to different probability distributions of the particle velocities. A standard grid for three dimensional motions of that kind, shown in Fig. 2, is called a D3Q19-grid, see [17] (D3: three dimensional Q19: 19 discrete velocities).

3 Test solutions

3.1 Underresolved DNS

DNS solutions need numerical grids that are fine enough to resolve the smallest scales involved. Quite generally these smallest scales are of the order of the Kolmogorov scale

$$\eta = \frac{\nu^{3/4}}{\varepsilon^{1/4}} \tag{5}$$

where ν is the kinematic viscosity of the fluid and ε is the local dissipation rate of the flow. This scale strongly depends on the Reynolds number (roughly $\eta \sim \mathrm{Re}^{-3/4}$) so that DNS solutions quite generally are restricted to relative small Reynolds numbers.

Since the main question of our study is about the large scales that occur in porous media flows we (in a first step) determine the size of the REV-T with so-called underresolved DNS solutions. These are solutions with numerical grids (Δx_i: step sizes) for which $\Delta x_i / \eta$ is larger than 1. The underlying assumption is that the large scale motion is not critically influenced by missing small scales. This assumption is supported by the generally small backscatter (energy transfer from small to large scales) in turbulent flow but nevertheless have to be verified in a later study with the final solutions on grids that meet the Kolmogorov scale condition.

3.2 Test cases 1 to 4

Taking into account the requirements with respect to the REV-T as well as the computer resources available to us for a preliminary calculation we selected test cases 1 to 4 with the parameters according to table 1. Quite generally we choose the obstacle size d as the geometrical unit scale and refer all geometric parameters to this d. Thus we do not fix the actual pore size but determine non-dimensional results. They can be interpreted as different cases by assigning different values to the length d, for example d=1mm or d=0.1mm. All values are possible as long as the Navier-Stokes equations (which are solved in the incompressible limit assuming no slip at the solid boundaries) are an adequate theoretical model for the flow.

As a first impression of the results Fig. 3 shows the turbulent structure of the flow in part of the solution

domain. Shown are surfaces of constant values Q=10. Details about this Q-value (which characterize and identify turbulent structures) as well as those about the two numerical methods employed are given in [14]. Fig. 3 shows that at least for this value of Q no large scale structures can be identified.

Table 1: Parameters of the test cases 1 to 4
d: unit length
$\mathrm{Re} = u_m d / \nu = 500$ for all cases

Test case	Pore size s	Domain size			Mesh resolution		
		L_1	L_2	L_3	M_1	M_2	M_3
1	2d	20d	20d	10d	280	280	140
2	2d	12d	8d	4d	168	112	56
3	2d	12d	4d	4d	168	56	56
4	2d	16d	16d	8d	640	640	320

3.3 Two-point correlations

One way to detect turbulent structures and analyze their scales is to determine two point correlations in the flow field. By this technique one looks at two quantities of the same kind in the flow field which are a certain distance $\vec{r}$ apart. When these quantities are subject to fluctuations (like in a turbulent flow) their fluctuations with respect to the corresponding time mean value $\langle \cdots \rangle$ will have positive and negative values alike.

When a is such a quantity we write $a = \langle a \rangle + a'$ with $\langle a' \rangle = 0$ as a consequence of this splitting into time mean and fluctuating parts. When two such fluctuating quantities a_1 and a_2 are considered we have $\langle a_1' \rangle = 0$ and $\langle a_2' \rangle = 0$ but it is an open question how $\langle a_1' a_2' \rangle$ behaves. When a_1 and a_2 are totally uncorrelated the chance of $a_1' a_2'$ to be positive or negative is the same and thus $\langle a_1' a_2' \rangle = 0$ holds. When, however, a physical correlation of whatever kind exists there will be a nonzero value of $\langle a_1' a_2' \rangle$ indicating this correlation.

This idea is behind the two-point correlations between the quantities $a_i'(\vec{x})$ and $a_i'(\vec{x} + \vec{r})$ at a certain time t also called two-point, one-time autocovariance, see [18], defined as

$$R_{ij}(\vec{r}, \vec{x}) = \left\langle a_i'(\vec{x}, t) a_j'(\vec{x} + \vec{r}, t) \right\rangle \tag{6}$$

When $u_1'(\vec{x}, t)$ and $u_1'(\vec{x} + \vec{r}, t)$ are correlated we get

$$R_{11}(\vec{r}, \vec{x}_1) = \left\langle u_1'(\vec{x}_1, t) u_1'(\vec{x}_1 + \vec{r}, t) \right\rangle \tag{7}$$

Fig. 4 shows such a correlation for test case 1, see table 1, and $\vec{x}_1 = (L_1/2, L_2/2, L_3/2)$, i.e. in the middle of the computational domain with $\vec{r}$ covering the whole domain. From the color coding it can be seen that there is a strong correlation next to the correlation point $\vec{x}_1$ but also one that is around each obstacle. This, however, turns out to be a *pseudo-correlation* due to the fact that a locally similar and in phase flow occurs around the individual obstacles, like it would happen in a purely laminar flow.

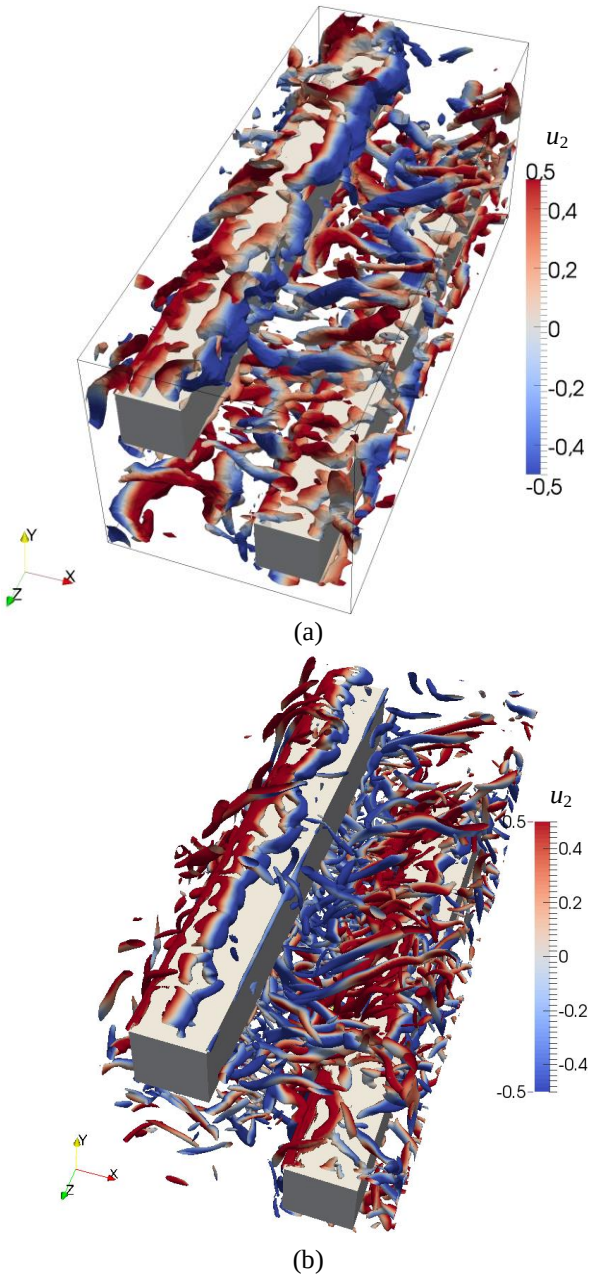

Fig. 3: Flow field details shown by iso-surfaces Q=10, (a): Case 1, FVM, (b): Case 4, LBM

The problem now is to distinguish this *pseudo-correlation* from the *turbulent correlation* we are interested in. For that purpose we introduce a two-point lateral correlation defined as

$$\tilde{R}_{11}(r_3, \vec{r}, \vec{x}_1) = \left\langle u_1'(\vec{x}_1, t) u_1'(\vec{x}_1 + \vec{r} + r_3 \vec{e}_3, t) \right\rangle \tag{9}$$

with $\vec{e}_3$ as unit vector in x_3-direction and $\vec{r}$ now being a vector within the (x_1, x_2) plane. Assuming that the pseudo-correlation in the regular porous medium of our test cases is the same on all levels $r_3 = const$ we can subtract $\tilde{R}_{11}$ from R_{11} and will get the turbulent

correlation provided r_3 is large enough. "Large enough" here means that the two correlation planes are far enough apart so that there will be no correlation due to large scale turbulent structures.

Fig. 5 shows $(R_{11} - \tilde{R}_{11})$ distributions for three values of r_3. In Fig. 5(a) with $r_3 = 0.2$ the lateral correlation $\tilde{R}_{11}$ obviously is affected by the large scale turbulent motion, so that $(R_{11} - \tilde{R}_{11})$ also depends on it. Once r_3 is large enough (Fig. 5(b) and (c)) there is no change in $(R_{11} - \tilde{R}_{11})$ anymore, obviously because r_3 exceeds the length scale of the largest turbulent structures. What is left is the turbulent correlation

$$\hat{R}_{11}(\vec{r}, \vec{x}_1) = R_{11}(\vec{r}, \vec{x}_1) - \tilde{R}_{11}(r_3 > r_{3c}, \vec{r}, \vec{x}_1) \qquad (9)$$

with r_{3c} being the critical value of r_3, up to which there is an influence of large scale structures.

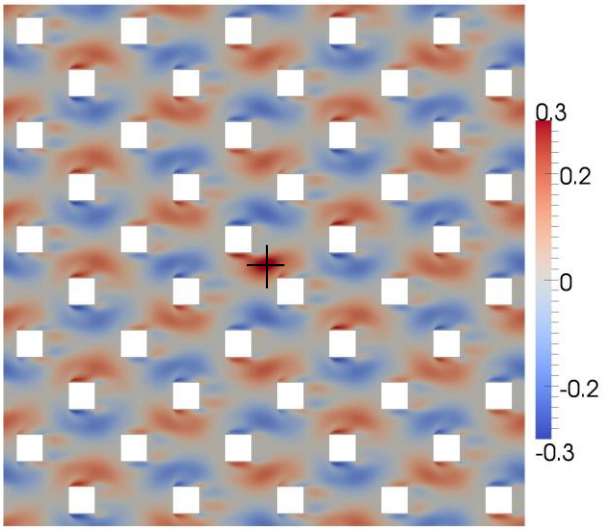

Fig. 4: Two point correlation R_{11} in the computational domain of test case 1, correlation point $\vec{x}_1$ marked by the cross in the middle

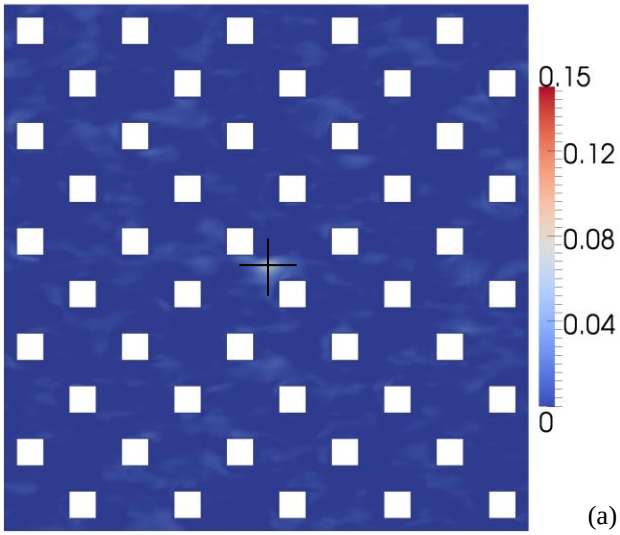

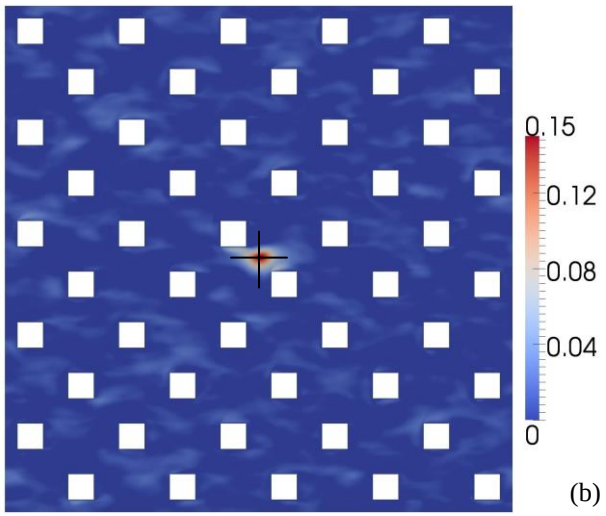

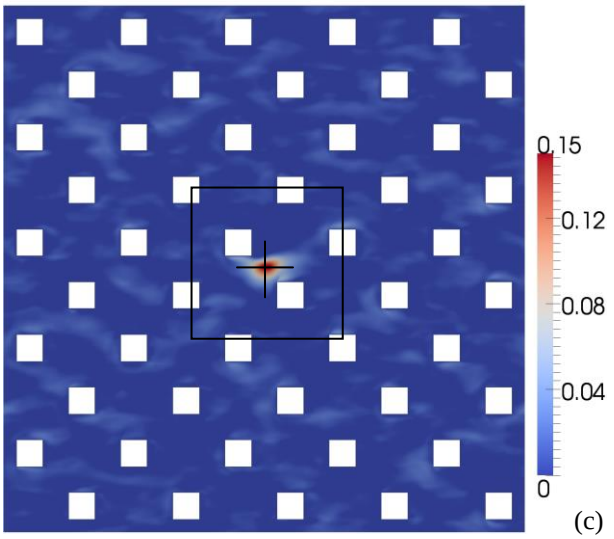

Fig. 5: Two point correlation $(R_{11} - \tilde{R}_{11})$ in the computational domain of test case 1, correlation point $\vec{x}_1$ marked by the cross in the middle. The zoomed contours inside the frame of Fig. 5a are shown in Fig. 6.

(a) $r_3 = 0.2d$

(b) $r_3 = 3.5d$

(c) $r_3 = 5d$

Fig. 6 shows three points within the flow field as correlation points with $\vec{x}_1$ of Fig. 4 and 5 being one of them. The iso-surfaces with the same value of $\hat{R}_{11}$ around them show the correlation extension is of the same order of magnitude so that point 1 used so far can further on be taken as a characteristic correlation point.

From Fig. 5 and 6 we draw (tentative) conclusion that large scale turbulent structures are restricted in size by the porous matrix and are of the order of the pore size. This definitely supports the first view mentioned in the INTRODUCTION which assumes that turbulence in dense porous media is restricted to turbulence within the pores.

In a more extensive study which is underway at the moment we are going to prove these tentative results by fully resolved DNS solutions. They need mesh resolution with up to 500 million grid points (in this study the maximum number of grid points was 130 million) and cpu times up to 100,000 hours (in the present study the maximum number of cpu hours was 30,000).

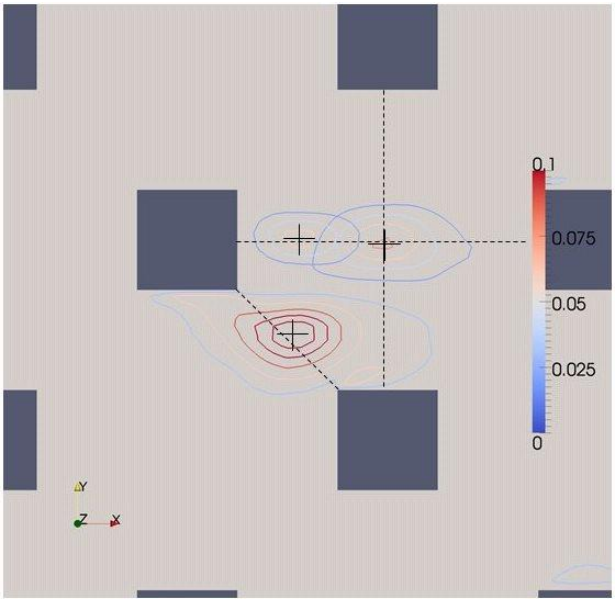

Fig. 6 Iso-surfaces of $\hat{R}_{11}$ at three points

CONCLUSIONS

Based on the (preliminary) results of our under-resolved DNS solutions we can tentatively conclude that turbulent structures in porous media flows are restricted in size to the scale of the pores. This conclusion can be drawn based on two-point turbulent correlations taking in account the effect of a pseudo correlation. This pseudo correlation is due to the regular structure of the generic porous matrix in our study.

ACKNOWLEDGEMENT

The authors gratefully acknowledge the support of this study by the DFG (Deutsche Forschungsgemeinschaft) and the HLRN (North-German Supercomputing Alliance).

REFERENCES

[1] Wibel, W., Ehrhard, P. (2006) Experiments on liquid pressure-drop in rectangular microchannels, subject to non-unity aspect ratio and finite roughness, In: Proceedings of Fourth International Conference on Nanochannels, Microchannels and Minichannels, Limerick, Ireland.

[2] Wibel, W., Ehrhard, P. (2009) Experiments on the laminar/turbulent transition of liquid flows in rectangular microchannels, Heat Trans. Eng. 30: 70-77.

[3] Nield, D.A. (1991) The Limitations of the Brinkman-Forchheimer Equation in Modeling Flow in a Saturated Porous Medium and at an Interface, Int. J. Heat Fluid Flow, 12: 269–272.

[4] Nield, D.A. (2001) Alternative models of turbulence in a porous medium, and related matters. ASME J. Fluids Engng. 123: 928-931.

[5] Lee, K.B., Howell, J. R. (1991) Theoretical and experimental heat and mass transfer in highly porous media. Int. J. Heat Mass Transfer 34: 2123-2132.

[6] Prescott, P.J., Incropera, F.P. (1995) The effect of turbulence on solidification of a binary metal alloy with electromagnetic stirring. ASME J. Heat Transfer, 117: 716-724.

[7] Antohe, B.V., Lage, J.L. (1997) A general two-equation macroscopic turbulence model for incompressible flow in porous media. Int. J. Heat Mass Transfer 40: 3013-3024.

[8] Moin, P. & Mahesh, K. (1998) Direct numberical simulation: a tool in turbulence research. Annu. Rev. Fluid Mech. 30: 539-538.

[9] Ma, X., Karamanos, G..-S. & Karniadakis, G.. E. (2000) Dynamics and low-dimensionality of a turbulent near wake. J. Fluid Mech. 410: 29-65.

[10] Parnaudeau, P., Carlier, J., Heitz, D. & Lamballais, E. (2008) Experimental and numerical studies of the flow over a circular cylinder at Reynolds number 3900, Phys. Fluids 20: 085101.

[11] Afgan, I, Kahil, Y. Benhamadouche, S. & Sagaut, P. (2011) Large eddy simulation of the flow around single and two side-by-side cylinders at subcritical Reynolds numbers. Phys. Fluids 23: 075101.

[12] Kis, P. Analyse turbulenter gemischter Konvektion auf der Basis von DNS-Daten, PhD dissertation, TU Hamburg-Harburg, Verlag Dr. Hut, München, ISBN 978-3-8439-0104-8, 2011.

[13] Jin, Y. & Herwig, H. (2014) Turbulent flow in channels with shark skin surfaces: Entropy generation and its physical significance, Int. J. Heat Mass Trans., 70: 10-22.

[14] Jin, Y. & Herwig, H. (2013) From single obstacles to wall roughness: some fundamental investigations based on DNS results for turbulent channel flow. Z. Angew. Math. Phys., 64: 1337-1352.

[15] Herwig, H. (2002) Strömungsmechanik, Springer-Verlag, Berlin.

[16] Aidun, C. K. & Clausen, J. R. (2009) Lattice-Boltzmann Method for Complex Flows. Annu. Rev. Fluid Mech. 41: 439-472.

[17] Succi, S. (2001) The Lattice Boltzmann Equation for Fluid Dynamics and Beyond (Oxford University Press).

[18] Pope, S. B. Turbulent flows (2000) Cambridge University press, Cambridge.